SPANDIDOS PUBLICATIONS

ONCOLOGY LETTERS 10: 2565-2568, 2015

Diagnostic utility of diffusion-weighted magnetic resonance imaging in two common renal tumors

ZHAOXIA WEN, ZHENCHAO SUN and YUXING WANG

Department of Radiology, Linyi People's Hospital, Linyi, Shangdong 276003, P.R. China

Received October 21, 2014; Accepted July 16, 2015

DOI: 10.3892/ol.2015.3605

Abstract. The aim of the present study was to evaluate the utility of diffusion-weighted magnetic resonance imaging (DWI) in the diagnosis of common renal tumors. Conventional magnetic resonance imaging and DWI were performed on 85 patients with renal lesions (54 renal carcinoma and 31 renal angiomyolipoma cases). The apparent diffusion coefficient (ADC) values in each case at b=800 sec/mm^2 were measured in the ADC maps using a statistical software package. The 54 cases of renal cell carcinoma showed a high signal intensity in the parenchyma, and the 31 renal angiomyolipoma cases showed a well-defined mixed signal intensity on DWI. The soft-tissue component showed a high signal intensity and the fat tissue showed a low signal intensity on DWI. When the b-value was set to 800 sec/mm^2, the mean ADC was significantly lower in the renal carcinoma cases than in the renal angiomyolipoma cases. In conclusion, the measurement of ADC on DWI can reveal the structure of renal tumors, which is beneficial in diagnosing and determining the prognosis of benign and malignant renal tumors.

Introduction

Renal cell carcinoma is the most common primary malignant tumor of the kidney, accounting for 85-90% of malignant kidney tumors (1) and 3% of all malignant tumors, with an incidence that is increasing yearly (2). Angiomyolipoma is the most common benign tumor of the kidney, comprising 7-9% of kidney tumors. The accurate evaluation of tumor behavior is critical in selecting an appropriate therapy and determining the prognosis. At present, the most commonly employed imaging modalities for renal tumors include computed tomography (CT), magnetic resonance imaging (MRI) and contrast-enhanced imaging. To differentiate between benign and malignant tumors or tumor stages, tissue density is measured on CT, the tissue signal intensity if measured on plain MRI and the pattern of contrast enhancement is examined on enhanced images. Renal angiomyolipoma usually contains significant fat and therefore, shows typical characteristics of fat on CT or MRI. The differential diagnosis of renal carcinoma is usually not difficult, but lesions with little or no fat and small tumors are difficult to discern on conventional CT, plain MRI and contrast-enhanced imaging (3-5). In addition, certain patients are allergic to the contrast material used during enhanced CT (6,7). Contrast-enhanced MRI may produce fewer allergic reactions, but it can also accelerate the progression of nephrogenic systemic fibrosis in patients with renal insufficiency (8-10).

With recent developments in imaging technology and the increased use of software for high-field MRI (1.5T and 3.0T), diffusion-weighted MRI (DWI) has gained wide use clinically. This diagnostic technique offers the advantage of good safety and does not require a contrast agent. DWI is the only non-invasive functional imaging able to assess the water diffusion status *in vivo*, and as a result, it is widely used in the examination of the central nervous system, particularly for the early diagnosis of cerebral infarction (11) and the staging of astrocytoma. The apparent diffusion coefficient (ADC) is an important index that is measured during DWI. In recent years, follow-up DWI has been increasingly employed in imaging the abdominal organs, breast, pancreas, liver and kidney (12-16). DWI provides functional information through three parameters: The dispersion diagram, the ADC diagram and the ADC value, which has gained significant attention due to its role in tumor diagnosis (17).

In the present study, a retrospective analysis was performed on 54 cases of renal carcinoma and 31 cases of angiomyolipoma assessed by DWI in order to investigate the utility of DWI in the differential diagnosis of common benign and malignant tumors in the kidney.

Materials and methods

General data. The complete medical records of 85 renal tumor cases presenting to the Linyi People's Hospital (Linyi, Shangdong, China) between March 2006 and December 2010 were collected. All patients underwent plain MRI and DWI pre-operatively, and the diagnosis was confirmed surgically by

Correspondence to: Dr Yuxing Wang, Department of Radiology, Linyi People's Hospital, 27 Jiefang Road, Linyi, Shangdong 276003, P.R. China
E-mail: yuxingwangcn@126.com

Key words: diffusion-weighted magnetic resonance imaging, renal cell carcinoma, renal angiomyolipoma, apparent diffusion coefficient

the Department of Urology. Among the 85 patients, 59 were male and 26 were female; the mean patient age was 53.8 years (range, 23-81 years). All 85 cases presented with unilateral renal tumors, 48 on the right and 37 on the left. The upper pole of the kidney was affected in 30 cases, the lower pole in 37 cases and the renal hilus in 18 cases. Clinical signs were absent in 38 cases, and in the remainder, the following physical findings were observed: Gross hematuria (n=14); lower back pain (n=13); lower back pain with hematuria (n=15); and a waist mass (n=5). Of the 54 cases of renal cell carcinoma, 8 patients underwent tumor enucleation, 37 patients underwent a nephrectomy and 9 patients underwent a radical nephrectomy. Of the 31 cases of renal angiomyolipoma, 4 patients underwent a nephrectomy and 27 patients underwent tumor enucleation. Tumors were diagnosed on post-operative histopathological staging as follows: Clear cell renal cell carcinoma (n=46); papillary carcinoma (n=7); chromophobe cell carcinoma (n=1); and renal angiomyolipoma (n=31). This study was conducted in accordance with the declaration of Helsinki and with approval from the Ethics Committee of Linyi People's Hospital. Written informed consent was obtained from all participants.

MRI examination. All 85 patients underwent plain MRI and DWI (1.5T; Twin Speed Infinity with Excite II; GE Healthcare Life Sciences, Pittsburgh, PA, USA). The patient was placed in the supine position and the phased array surface coil was positioned at the abdomen, with the Torso PA coils at the abdominal wall and side. The abdominal wall was secured in front of the coil using a bandage, and patients were trained to breathe deeply prior to holding their breath in order to reduce motion artifacts during scanning. Axial MRI was performed in a fast recovery fast spin echo (SE) accelerated sequence [axial T1-weighted imaging (WI), T2WI and fat suppression] and a coronal fast imaging employing steady state acquisition sequence. A single-shot SE echo planar imaging was obtained during axial DWI scanning. The two scans were performed with the same body position, and layer thickness on axial T2WI, and imaging parameters were as follows: b=0 or 800 sec/mm^2; stimulated repetition time/echo time of 4,000/56 msec one time; received bandwidth of 125 kHz; thickness/distance of 5/0 mm; field of view of 36x34 cm; and a matrix of 128x128 cm. Sensitive gradient pulses were applied in the X-, Y- and Z-axes. Patients were required to breath-hold during scanning.

Image transmission. The DWI images were transferred to an AW4.0 workstation and processed using FuncTool 2.0 software (both GE Healthcare Life Sciences).

Image processing. During processing, the threshold was defined by removing fat, bone and gas regions from the image, and the b-value was entered, resulting in the DWI and ADC maps.

The region of interest (ROI) measured 60-100 mm^2. Using the conventional axial T2WI and DWI images as a reference, the ROI was set at the same size in three successive levels of the ADC diagram, and the ADC was measured. The mean value was designated as the final value. In lesions with a homogeneous signal, the ROI avoided the margins as much as possible in order to reduce the partial volume effect. In lesions with an inhomogeneous signal, the ROI was positioned in the solid region of the lesion, and cystic change, necrosis, hemorrhage and calcification areas were avoided when possible.

The ADC values were measured and recorded, and the ADC diagram was stored. The ADC was calculated according to the following formula: ADC = (S0 / S1) / (b1 - b0), where b0 was 0 sec/mm^2, b1 was 800 sec/mm^2, S0 was the DWI signal intensity at a b-value of 0 sec/mm^2 and S1 was the DWI signal strength with a b-value of 800 sec/mm^2.

Statistical analysis. The normal distribution of ADC values was evaluated in the renal cell carcinoma group and the renal angiomyolipoma group using SPSS14.0 statistical analysis software (SPSS, Inc., Chicago, IL, USA). Subsequent to confirming that the data were normally distributed, the mean ADC values were compared between the two groups using an analysis of variance. $P<0.05$ was considered to indicate a statistically significant difference.

Results

MRI, DWI, and ADC in the renal angiomyolipoma group. On T1WI, the 31 angiomyolipoma cases showed a high partial fat signal intensity and a low signal intensity in the soft tissue. When the fat signal was suppressed, it showed a low signal intensity on T2 images, while the soft tissues showed a slightly high signal intensity. The corresponding DWI image showed a lower fat signal intensity and slightly higher signal intensity for soft tissue; the fat signal intensity on the pseudo-color ADC map was high, the soft tissue was slightly low and the signal intensity was inhomogeneous (Fig. 1A).

MRI, DWI and ADC in the renal cell carcinoma group. Among the 54 renal cell carcinoma cases, 18 cases showed a homogeneous low signal intensity on T1WI images, a homogeneous high signal intensity on T2WI and a homogeneous high signal intensity on DWI. The corresponding pseudo-color ADC map showed a slightly low signal intensity and a uniform signal strength. In 36 cases containing necrosis, cystic change or hemorrhage, the T1WI showed an inhomogeneous low signal intensity, and the T2WI and DWI showed an inhomogeneous high signal intensity. The corresponding pseudo-color ADC map showed a heterogeneous slightly low signal intensity (Fig. 1B).

ADC comparison. As detailed in Table I, the ADC for the renal cell carcinoma group was significantly lower than that in the renal angiomyolipoma group ($P<0.05$).

Discussion

The present study demonstrated that the ADC in renal cell carcinoma is lower than that in renal angiomyolipoma, which is consistent with the results of studies by Doğanay *et al* (18), Mytsyk *et al* (19) and Zhang *et al* (20), which found that the ADC was lower in malignant kidney tumors than in benign tumors. Doğanay *et al* reported a mean ADC of $2.21\pm0.63\times10^{-3}$ mm^2/sec for renal cell carcinoma and $2.55\pm0.49\times10^{-3}$ mm^2/sec for benign tumors. Mytsyk *et al*

Table I. Comparison of the ADC in the renal cell carcinoma and renal angiomyolipoma groups when the b-value was set at 800 sec/mm^2.

Group	n	ADC, x10^{-3} mm^2/sec	F	P-value
Renal angiomyolipoma	31	1.8271±0.3486	25.718	0.000
Renal carcinoma	54	1.4181±0.1643		

ADC, apparent diffusion coefficient.

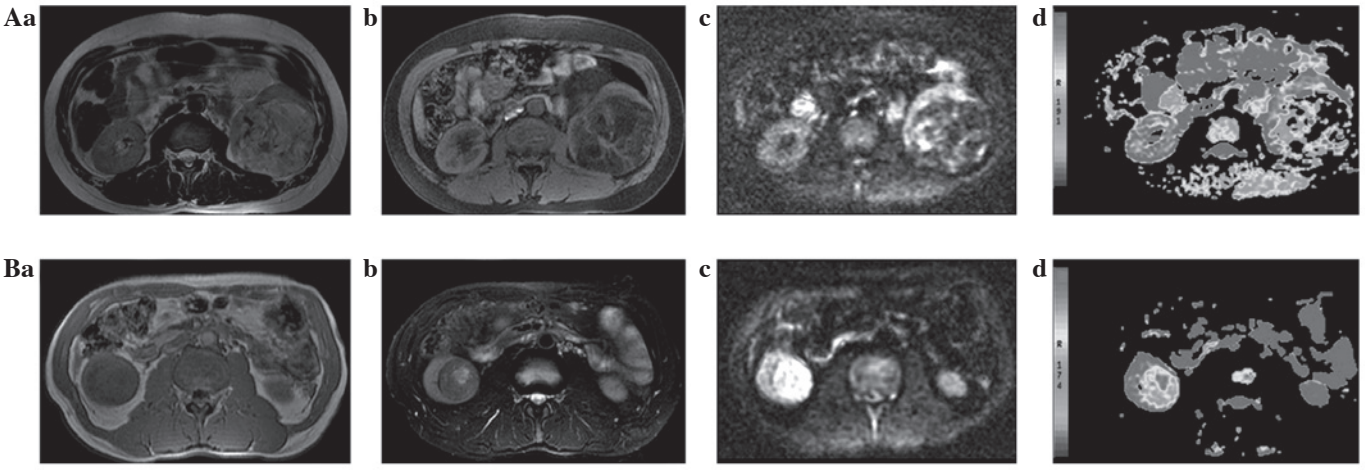

Figure 1. Map of MRI scan, DWI and ADC of (A) renal vascular leiomyoma group and renal cell carcinoma and (B) renal cell carcinoma groups. (a) T1WI and (b) T2WI images, and (c) T2WI and (d) ADC maps. MRI, magnetic resonance imaging; DWI, diffusion-weighted MRI; ADC, apparent diffusion coefficient; WI, weighted imaging.

reported a similar trend of 2.11±0.25x10^{-3} mm^2/sec in renal cell carcinoma and 2.36±0.32x10^{-3} mm^2/sec in angiomyolipoma. Zhang *et al* reported a mean ADC of 1.264±0.271x10^{-3} mm^2/sec for renal cell carcinoma and 1.717±0.431x10^{-3} mm^2/sec for angiomyolipoma. The present analysis showed a mean ADC of 1.4181±0.1643x10^{-3} mm^2/sec for renal cell carcinoma and 1.8271±0.3486x10^{-3} mm^2/sec for renal angiomyolipoma.

The diagnosis of tumors on DWI is based on organizational, structural, cell density and karyoplasmic ratio changes within lesions, as well as changes to the large molecular distribution in the intra- and extracellular spaces; these variations alter the Brownian motion of water molecules, generating an abnormality in the DWI signal (21). The cell concentration increases in renal cell carcinoma, which decreases the extracellular clearance and slows the extracellular water molecular motion (22). In addition, the cell nuclei are relatively larger and the cytoplasm lessened, which further reduces water molecular motion within cells. These mechanisms explain the lower ADC value in renal cell carcinoma compared with normal tissues. The ADC is an index that measures the magnitude of random molecular motion within a given volume and is calculated as follows: ADC = ln(low S / high S) / (high b - low b), where low S and high S represent the signal intensity measured by DWI corresponding to a low b and high b, respectively, and b is a diffusion gradient factor. By calculating the ADC at each voxel and arranging the results in a grayscale image, an ADC diagram can be generated, providing a map of the ADCs of the entire lesion. In the ADC map, high signal areas represent high dispersion; the ADC value is high, while the signal on the corresponding DWI map is low. By contrast, a low signal zone on the ADC map represents a low dispersion region, indicating a low ADC value and a high signal on the corresponding DWI map. In addition, the ADC map eliminates the effect of T2 transmission and does not depend on the strength of the magnetic field and gradient; thus, the ADC value reflects the magnitude of molecular water movement in tissues, and can be measured and compared graphically (23).

The present study has two notable limitations. Firstly, the majority of the renal angiomyolipomas contained significant amounts of fat, and only a few lesions contained little or no fat. Furthermore, other common benign renal tumors, such as renal oncocytoma, were not included in this small study.

This study indicates that DWI may be valuable in the differential diagnosis of benign and malignant renal tumors in the kidney; it can differentiate between benign and malignant tumors, and could prove particularly useful for small renal vascular leiomyoma, tumors with little to no fat and renal cell carcinoma. DWI should be considered an important supplementary tool in the diagnosis and differentiation of renal tumors.

References

1. Lam JS, Shvarts O and Pantuck AJ: Changing concepts in the surgical management of renal cell carcinoma. Eur Urol 45: 692-705, 2004.

2. Kirkali Z and Öber C: Clinical aspects of renal cell carcinoma. EAU Update Series 1: 189-196, 2003.
3. Fujii Y, Komai Y, Saito K, Iimura Y, Yonese J, Kawakami S, Ishikawa Y, Kumagai J, Kihara K and Fukui I: Incidence of benign pathologic lesions at partial nephrectomy for presumed RCC renal masses: Japanese dual-center experience with 176 consecutive patients. Urology 72: 598-602, 2008.
4. Jeon HG, Lee SR, Kim KH, Oh YT, Cho NH, Rha KH, Yang SC and Han WK: Benign lesions after partial nephrectomy for presumed renal cell carcinoma in masses 4 cm or less: Prevalence and predictors in Korean patients. Urology 76: 574-579, 2010.
5. Xiong YH, Zhang ZL, Li YH, Liu ZW, Hou GL, Liu Q, Yun JP, Zhang XQ and Zhou FJ: Benign pathological findings in 303 Chinese patients undergoing surgery for presumed localized renal cell carcinoma. Int J Urol 17: 517-521, 2010.
6. Loh S, Bagheri S, Katzberg RW, Fung MA and Li CS: Delayed adverse reaction to contrast-enhanced CT: A prospective single-center study comparison to control group without enhancement. Radiology 255: 764-771, 2010.
7. Katzberg RW and Newhouse JH: Intravenous contrast medium-induced nephrotoxicity: Is the medical risk really as great as we have come to believe? Radiology 256: 21-28, 2010.
8. Marckmann P, Skov L, Rossen K, Dupont A, Damholt MB, Heaf JG and Thomsen HS: Nephrogenic systemic fibrosis: Suspected causative role of gadodiamide used for contrast-enhanced magnetic resonance imaging. J Am Soc Nephrol 17: 2359-2362, 2006.
9. Deo A, Fogel M and Cowper SE: Nephrogenic systemic fibrosis: A population study examining the relationship of disease development to gadolinium exposure. Clin J Am Soc Nephrol 2: 264-267, 2007.
10. Abu-Alfa AK: Nephrogenic systemic fibrosis and gadolinium-based contrast agents. Adv Chronic Kidney Dis 18: 188-198, 2011.
11. Artz NS, Sadowski EA, Wentland AL, Grist TM, Seo S, Djamali A and Fain SB: Arterial spin labeling MRI for assessment of perfusion in native and transplanted kidneys. Magn Reson Imaging 29: 74-82, 2011.
12. Irie H, Kamochi N, Nojiri J, Egashira Y, Sasaguri K and Kudo S: High b-value diffusionweighted MRI in differentiation between benign and malignant polypoid gallbladder lesions. Acta Radiol 15: 236-240, 2011.
13. Chandarana H, Lee VS, Hecht E, Taouli B and Sigmund EE: Comparison of biexponential and monoexponential model of diffusion weighted imaging in evaluation of renal lesions: Preliminary experience. Invest Radiol 46: 285-291, 2011.
14. Rheinheimer S, Stieltjes B, Schneider F, Simon D, Pahernik S, Kauczor HU and Hallscheidt P: Investigation of renal lesions by diffusion-weighted magnetic resonance imaging applying intravoxel incoherent motion-derived parameters-initial experience. Eur J Radiol 81: e310-e316, 2012.
15. Sandrasegaran K, Sundaram CP, Ramaswamy R, Akisik FM, Rydberg MP, Lin C and Aisen AM: Usefulness of diffusion-weighted imaging in the evaluation of renal masses. AJR Am J Roentgenol 194: 438-445, 2010.
16. Baliyan V, Das CJ, Sharma S and Gupta AK: Diffusion-weighted imaging in urinary tract lesions. Clin Radiol 69: 773-782, 2014.
17. Chen S, Ikawa F, Kurisu K, Arita K, Takaba J and Kanou Y: Quantitative MR evaluation of intracranial epidermoid tumors by fast fluid-attenuated inversion recovery imaging and echo-plannar diffusion-weighted imaging. AJNR Am J Neuroradiol 22: 1089-1096, 2001.
18. Doğanay S, Kocakoç E, Ciçekçi M, Ağlamiş S, Akpolat N and Orhan I: Ability and utility of diffusion-weighted MRI with different b values in the evaluation of benign and malignant renal lesions. Clin Radiol 66: 420-425, 2011.
19. Mytsyk Y, Borys Y, Komnatska I, Dutka I and Shatynska-Mytsyk I: Value of the diffusion-weighted MRI in the differential diagnostics of malignant and benign kidney neoplasms-our clinical experience. Pol J Radiol 79: 290-295, 2014.
20. Zhang YL, Yu BL, Ren J, Qu K, Wang K, Qiang YQ, Li CX and Sun XW: EADC values in diagnosis of renal lesions by 3.0 T diffusion-weighted magnetic resonance imaging: Compared with the ADC values. Appl Magn Reson 44: 349-363, 2013.
21. Zimmerman RD: Is there a role for diffusion-weighted imaging in patients with brain tumors or is the 'bloom off the rose'? AJNR Am J Neuroradiol 22: 1013-1014, 2001.
22. Wang J, Takashima S, Takayama F, Kawakami S, Saito A, Matsushita T, Momose M and Ishiyama T: Head and neck lesions: Characterization with diffusion-weighted echo-planar MR imaging. Radiology 220: 621-630, 2001.
23. Huisman TA: Diffusion-weighted imaging: Basic concepts and applicationin cerebral stroke and head trauma. Eur Radiol 13: 2283-2297, 2003.